https://doi.org/10.15360/1813-9779-2026-3-2682

Post-Ischemic Long-Term Neuronal Changes in the Sensorimotor Cortex in the Experimental Setting

Viktor A. Akulinin[1]*, Sergei S. Stepanov[1], Kirill S. Tagakov[1], Vladislav I. Sergeev[1], Dmitry B. Avdeev[1], Galina U. Zhanaidarova[2], Dmitry V. Akulinin[3], Anastasia Yu. Shoronova[1], Irina G. Tsuskman[1]

[1] Omsk State Medical University, Ministry of Health of Russia, 12 Lenin Str., 644099 Omsk, Russia
[2] Karaganda Medical University, 40 Gogolya Str.,100008 Karaganda, Republic of Kazakhstan
[3] Plekhanov Russian University of Economics, 36 Stremyanny Lane, 109992 Moscow, Russia

For citation: *Viktor A. Akulinin, Sergei S. Stepanov, Kirill S. Tagakov, Vladislav I. Sergeev, Dmitry B. Avdeev, Galina U. Zhanaidarova, Dmitry V. Akulinin, Anastasia Yu. Shoronova, Irina G. Tsuskman.* Post-Ischemic Long-Term Neuronal Changes in the Sensorimotor Cortex in the Experimental Setting. *Obshchaya Reanimatologiya = General Reanimatology.* 2026; 22 (3): 28–40. https://doi.org/10.15360/1813-9779-2026-3-2682 [In Russ. and Engl.]

***Correspondence to:** Victor A. Akulinin, v_akulinin@outlook.com

Summary

The aim of the study was to identify the characteristics of dynamic reactive neuronal changes in sensorimotor cortex (SMC) layers III and V of the rat brain in the remote period (up to 270 days) following bilateral common carotid arteries ligation (CCAL).

Methods. The experiment was conducted on 66 male Wistar rats (a prospective cohort study with sequential terminal outcomes): intact control ($n=6$) and groups with survival at 30, 90, 150, 210, and 270 days post-bilateral CCAL ($n=6$ in each group after adjusting for mortality). Histological methods (Nissl and hematoxylin-eosin staining) were used to assess the total neuronal numerical density (NND), the density of four types of reactive altered cells (hyperchromatic shriveled cells — HCSC; hyperchromatic non-shriveled cells — HCNSC; hypochromatic cells — HCC; shadow cells — SC) and the neuroglial index (NGI). Paired and multiple comparison methods, linear mixed models (LMM) with random intercept for the animal (to account for the paired data structure), Jonckheere–Terpstra test, quadratic trend test, correlation analysis, and △-analysis were applied.

Results. A biphasic reduction in NND was observed in layer III of the SMC (maximum of -44.6% at 30 days, $p<0.001$) with a wave-like dynamics (quadratic trend: $F=16.4$, $p<0.001$). HCNSC peak at 30 days (+683%) followed by a decrease, while HCC showed a delayed peak at 150 days (+500%); both parameters showed a mixed pattern (steadily increasing trend: $Z=1.88$, p=0.030 for HCNSC; $Z=2.45$, $p=0.007$ for HCC; quadratic component: $F=8.2$ and 7.4, $p<0.01$). SCs demonstrated non-monotonous dynamics (quadratic trend: $F=19.2$, $p<0.001$) with a delayed peak at 210 days. NGI peaked at 30 days (transient gliosis, +95.5%, steadily decreasing trend, $Z=-4.92$, $p<0.001$). The decrease in NND was less pronounced in layer V of the SMC, (–11.6% at 150 days, $p=0.048$), but there was an extreme increase in HCSC at 30 days (+945% from control, with a continuously decreasing trend, $Z=-2.94$, $p=0.002$), a monotonous depletion of HCC (linear increasing trend, $Z=4.82$, $p<0.001$), and a prolonged building up gliosis (NGI +42% by 270 days, mixed pattern: steadily increasing trend $Z=4.15$, $p<0.001$; quadratic component $F=5.1$, $p=0.028$). LMM confirmed a significant «Layer × Time» interaction for all parameters ($F=24.1$–71.2; $p<0.001$). A correlational analysis revealed moderate positive correlations between the layers (for SCs: $r=0.58$; $r\_partial=0.52$; $p=0.004$; for HCSC: $r=0.52$; $p=0.008$; for NGI: $r=0.44$; $p=0.016$). The △-analysis showed consistency in changes for SC, HCSC, and NGI. The extremum moments for SC (210 days) and HCSC (30 days) were synchronous in both layers. Temporal precedence of layer III was found for NGI (early peak of gliosis at 30 days compared to 270 days in layer V), as well as for HCSC and HCC (30–150 days compared to 90 days in layer V). Temporal precedence of layer V was identified for the first peak of SC (90 days compared to 210 days in layer III).

Conclusion. Chronic ischemia induces various damage scenarios: layer III is characterized by a biphasic reduction in NND, asynchronous peaks of HCSC (30 days) and HCC (150 days), a delayed SC peak (210 days), and transient gliosis (a model of damage with delayed degeneration); layer V exhibits an extreme early increase in HCSC (30 days), early peak of SC (90 days), and prolonged gliosis (a model of progressive degeneration). Correlation and △-analysis indicate moderate synchrony in the degeneration processes; no convincing evidence of cascading damage propagation from superficial layers to deeper ones was obtained.

Keywords: chronic cerebral ischemia; sensorimotor cortex; cortical layers; hyperchromatic neurons; shadow cells; neuroglial index; white rats

Conflict of interest. The authors declare no conflict of interest.

Information about the authors:
Viktor A. Akulinin: https://orcid.org/0000-0001-6097-7970
Sergei S. Stepanov: https://orcid.org/0000-0003-0741-3337
Kirill S. Tagakov: https://orcid.org/0000-0002-8310-896X

Vladislav I. Sergeev: https://orcid.org/0000-0002-5878-7403
Dmitry B. Avdeev: https://orcid.org/0000-0003-4976-7539
Galina U. Zhanaidarova: https://orcid.org/0000-0003-1143-4843
Dmitry V. Akulinin: https://orcid.org/0009-0002-4208-2748
Anastasia Y. Shoronova: https://orcid.org/0000-0002-6362-3796
Irina G.Tsuskman: https://orcid.org/0000-0003-3667-7905

Introduction

Chronic cerebral ischemia (CCI) is a key pathophysiological factor in cerebral insufficiency and underlies discirculatory encephalopathy and vascular cognitive impairment, which represent one of the most significant medical and social challenges in neurology [1, 2]. The pathophysiology of CCI is based on prolonged hypoperfusion, leading to a complex of metabolic disruptions, oxidative stress, neuroinflammation, and, ultimately, neuronal death and glial activation [3, 4]. Despite significant progress in understanding the general mechanisms of ischemic injury, layer-specific vulnerability of various cortical regions during prolonged hypoperfusion remains insufficiently studied.

The sensorimotor cortex, as an integrative region, plays a critical role in the organization of voluntary movements and processing of somatosensory information, therefore level of its dysfunction directly correlates with the clinical presentation of motor and sensory disorders in cerebrovascular disease [5]. Cortical architecture is organized in layers with unique cyto- and chemoarchitectonics, neuronal composition, and connection patterns in each layer, which determine their functional specialization and, likely, differences in resistance to damaging factors [6]. Thus, the large pyramidal neurons of layer V, which give rise to the corticospinal tract, are characterized by a high level of metabolic activity and may be highly sensitive to energy deficiency [7]. At the same time, neurons in layer III, which form corticocortical associative connections, may be secondarily affected due to disruptions in neural networks and trophic support [8]. Data from experimental studies on models of acute focal ischemia (middle cerebral artery occlusion) do indeed indicate the heterogeneity of damage to cortical layers involving both neurons and glial cells [9]. However, the dynamics of reactive and degenerative changes in specific cortical layers in the long term following the onset of chronic hypoperfusion, which mimics progressive vascular pathology in humans, have been described only fragmentarily.

One of the widely used experimental models for studying CCI is the bilateral common carotid artery ligation (2-vessel, 2VO — 2 vessels occlusion) model in rodents, which leads to a sustained reduction in cerebral blood flow and the development of delayed neurodegenerative changes [10]. Analysis of specific pathomorphological markers resulting from reactive neuronal changes (hyperchromia, shrinkage, chromatolysis), and emergence of shadow cells allows for the assessment not only of the extent of damage but also of the adaptive potential of neural tissue, as well as the dynamics of the neurodegenerative process [11]. The accompanying glial reaction, quantitatively assessed via the neuroglial index, is an integral component of pathomorphosis, it can be either protective or destructive in nature, depending on the timing and context [12].

It has been hypothesized that different cortical layers exhibit not only quantitative but also qualitative differences in the pathomorphological responses to chronic ischemia, which may reflect distinct mechanisms of vulnerability and adaptation.

The aim of this study was to identify the characteristics of the dynamics of neuronal responses in layers III and V of the sensorimotor cortex (SMC) of the rat brain at long-term intervals (up to 270 days) following bilateral common carotid arteries ligation (CCAL).

Materials and Methods

The study was conducted on 66 sexually mature male Wistar rats (weighing 250–300 g). The experiment was designed as a prospective cohort study with sequential terminal removal of animals. The animals were divided into 6 groups: an intact control group (n=6, not subjected to surgery) and 5 experimental groups with survival times of 30, 90, 150, 210, and 270 days (study time points) following bilateral CCAL.

To ensure 6 viable animals for analysis at each time point, the initial cohort size was calculated (n=11) taking into account the projected perioperative mortality (≈25%) and long-term mortality (≈20%). The experiment included 66 animals (11 in each of the 5 experimental groups + 6 intact controls). Perioperative mortality (first 7 days) was 23.6% (13 of 55 operated rats), primarily due to cerebral edema and ischemic respiratory failure. In the long-term period (8–270 days), another 17 animals (30.9% of those surviving the surgery) died due to progressive cachexia and infectious complications. The analyzed groups (n=6 for each time point) were formed from animals that reached the planned time point and were suitable for histological examination. The experiment was approved by the Local Ethics Committee at Omsk State Medical University (Protocol No. 11 dated September 16, 2022).

Under general anesthesia (Zoletil 100, 10 mg/kg, intramuscularly), a model of incomplete global ischemia was induced by irreversibly ligating both common carotid arteries. The neurovascular

bundles were dissected sequentially, both common carotid arteries were exposed, and two ligatures were applied to each artery at a distance of 2–3 mm from one another. Control animals were not subjected to surgery.

Animals were euthanized by perfusion of 30 mL of a 4% paraformaldehyde solution in phosphate buffer (pH 7.2–7.4) through the aorta at a pressure of 90–100 mm Hg. The brain was embedded in paraffin. The sensorimotor cortex was isolated using stereotaxic atlases. Sections 7 μm thick were stained with Nissl's thionin and hematoxylin-eosin. The following were assessed: total numerical neuronal density (NND, cells/mm²); the density of four types of reactively altered neurons: (hyperchromatic shriveled cells — HCSC; hyperchromatic non-shriveled cells — HCNSC; hypochromatic cells — HCC; shadow cells — SC and the neuroglial index (NGI) — the ratio of the number of glial cells to the number of neurons. Histological sections were examined under a Leica DM 1000 microscope (Leica Microsystems, Germany). For each animal in layers III and V of the SMC, 5 fields of view were analyzed (×40 objective, 0.2 mm²). For each parameter, the arithmetic mean across the 5 fields was calculated for each animal, yielding an individual value (animal-level). Next, for each experimental group (n=6), a variation series was formed from the individual values. Total sample size: for intra-layer analysis — 6 animals per group; for inter-layer comparisons — 6 pairs per time point; for correlation analysis — 36 animals (all time points); for △-analysis — 80 pairs of changes.

Statistical analysis was performed in *R* (version 4.3.2) using the tidyverse, lme4, lmerTest, emmeans, rstatix, and ARTool packages. For each parameter, the mean and standard error ($M \pm SEM$), median, and interquartile range (Me [$Q1$; $Q3$]) were calculated. Normality was tested using the Shapiro–Wilk test. Since layers III and V were measured in the same animal (paired data), linear mixed models (LMMs) with a random intercept for the «Animal» factor were used for the two-factor analysis. Effective degrees of freedom were estimated using the Satterthwaite method. When the residuals were non-normal, the Oshima–Algina rank transformation (ART, related to aligned ranks transformation 0 ART anova) was applied, followed by an LMM on the ranks. Analysis of temporal trends (monotonic trend): Jonckheere–Terpstra test. Non-monotonic (quadratic) trend: test for a quadratic component in Kruskal–Wallis rank-order ANOVA with orthogonal polynomials. A correlation analysis was performed. Correlations were calculated at the level of individual animals (n=36) using Pearson's coefficient and partial correlations (with the control of «Time» factor). To assess the consistency of the direction of parameter changes between adjacent time points, △-analysis was applied, and a comparison of the moments of parameter extrema in layers III and V of the rat brain's SMC was also performed. △-analysis was based on pseudo-individual trajectories formed by randomly pairing individual animals from independent terminal cohorts (30→90, 90→150, 150→210, 210→270 days). For this reason, this approach was considered exploratory and was not classified as a full-fledged equivalent of lag modeling.

The effective sample size was 80 unique pairs (4 transitions × 20 random pairings without repetition in a single iteration). A significance level of $\alpha = 0.05$ was adopted. Correction for multiple comparisons was performed using the Bonferroni method.

Results

In the control group, typical normochromatic pyramidal neurons predominated in layers III and V of the rat brain SMC. When stained with hematoxylin-eosin, they appeared as pyramidal or pear-shaped cells with a perikaryon diameter ranging from 15–25 μm (in layer III of the SMC) to 20–35 μm (in layer V of the SMC), with a central bright, rounded nucleus (8–12 μm) and a distinct dark-purple nucleolus; the pink eosinophilic cytoplasm had a granular structure due to uniformly distributed basophilic clumps of Nissl bodies. A distinct apical dendrite extended from the cell apex toward the surface of the cortex. Among the normochromatic cells, isolated, non- shriveled hyperchromatic neurons were noted (Fig. 1).

Throughout the entire observation period (30–270 days) following bilateral CCAL, various types of reactively altered neurons were detected in the SMC. Hematoxylin-eosin staining revealed polymorphism in the reactive changes of SMC neurons, reflecting prolonged hypoperfusion and compensatory-adaptive processes. However, the proportion of reactively altered neurons was significantly lower than in acute ischemia. The following types of altered neuronal cells were identified: 1) hyperchromatic non-shrunken cells (HCNSC), 2) hyperchromatic shriveled cells (HCSC), 3) hypochromic (HCC), 4) vacuolated, 5) shadow cells (SC), 6) phagocytosed, 7) atrophic (simplified), 8) hypertrophied (complex) (Fig. 2).

Long-term follow-up after permanent occlusion of both common carotid arteries revealed polymorphism in the reactive changes of neurons in the sensorimotor cortex, as detected by hematoxylin-eosin staining. Atrophically altered neurons were identified, characterized by reduced perikaryon size, a flattened pyramidal shape, a thinned apical dendrite, moderately basophilic cytoplasm, and a compact but structurally intact nucleus. Concurrently, hypertrophied neurons were recorded, characterized by an increase in perikaryon size, intense cytoplasmic basophilia, and a hypertrophied nucleolus.

Hyperchromatic, abnormally shrunken, shriveled (pyknomorphic) neurons represented cells at

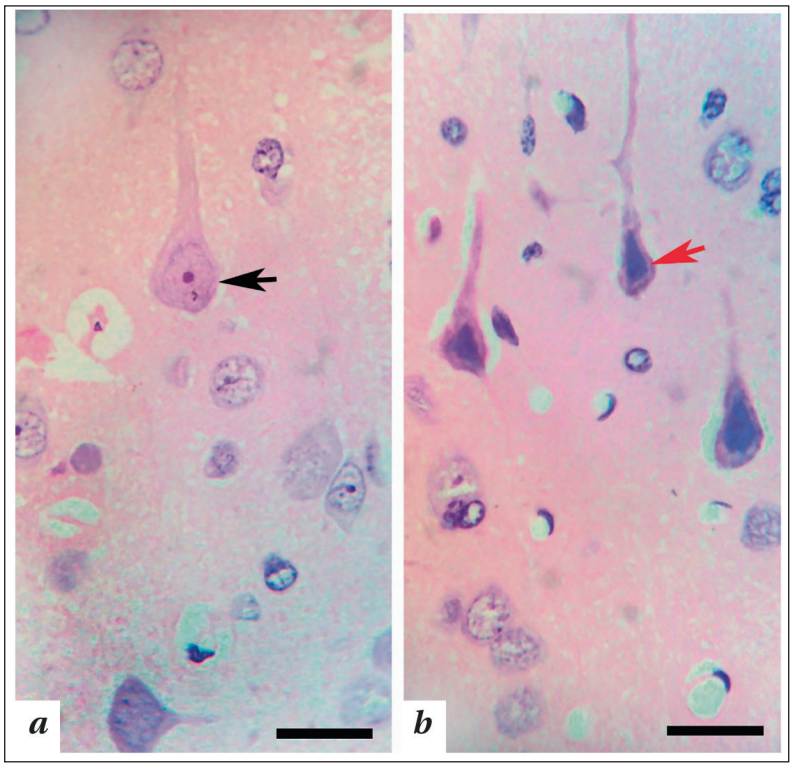

Fig. 1. Pyramidal neurons in layer V of the sensorimotor cortex of rats in the control group.
Note. Black arrow — normochromatic; red arrow — hyperchromatic, non- shriveled neurons. Hematoxylin-eosin staining (*a*, *b*). 100× objective, scale bar — 20 μm.

various stages of coagulative necrosis: with markedly reduced, angular perikarya and homogeneous, intense basophilia of the cytoplasm and nuclei, which was a consequence of critical hypoxia episodes. A sign of severe hydropic dystrophy under conditions of persistent metabolic stress was vacuolated neurons, whose cytoplasm contained multiple optically empty vacuoles, indicating edema and swelling of organelles (mitochondria, endoplasmic reticulum). «Shadow cells» with nearly complete lysis of the perikaryon indicated the complete loss of neurons in areas of maximum damage.

The presence of neurons with ischemic changes («red neurons»), characterized by eosinophilic cytoplasm and pyknotic nuclei, indicated the occurrence of acute episodes of hypoxia in a scenario of chronic hypoperfusion. Neurons with signs of chromatolysis were also noted, reflecting reactive changes associated with ribonucleoproteins degeneration.

The background changes consisted of diffuse and focal gliosis (with a predominance of activated microglia) and spongiosis (exhaustion and vacuolization of the neuropil). Against this altered background, reactively transformed neurons were arranged chaotically, forming areas of thinning and patterns of neuronophagy.

Morphometric analysis showed biphasic change in the NND in layer III of the SMC: a 44.6% decrease from the control level by day 30 ($p<0.001$), followed by an increase by days 150–210 and a subsequent decrease by day 270 (28.0% below control, $p<0.001$) (Tables 1, 2; Fig. 3). In layer V of the SMC, the decrease in NND was less obvious: the maximum drop of 11.6% was observed at day 150 ($p=0.048$) (Table 3). The accumulation of hyperchromic shrunken neurons was more pronounced in layer V. For the remaining parameters (HCNSC, HCC, SC, NGI), layer III demonstrated greater vulnerability (Table 3).

Table 3 presents the maximum deviation of each morphometric parameter from the reference values, expressed as a percentage, as well as the vulnerability ratio (the maximum change in layer V divided by the maximum change in layer III). A ratio greater than 1 indicates greater sensitivity in

Table 1. Results of a multiple intergroup comparison of morphometric parameters within each layer (intact control and time points 30, 90, 150, 210, and 270 days after ligation of the common carotid arteries).

Layer	Parameter	Criterion	Statistics	df	*p*
III	NND	Kruskal–Wallis	$H=29.2$	5	<0.001
	HCSC	ANOVA	$F=52.4$	5.30	<0.001
	HCNSC	Kruskal–Wallis	$H=28.8$	5	<0.001
	HCC	Kruskal–Wallis	$H=29.5$	5	<0.001
	SC	Kruskal–Wallis	$H=27.1$	5	<0.001
	NGI	ANOVA	$F=98.2$	5.30	<0.001
V	NND	Kruskal–Wallis	$H=17.6$	5	0.003
	HCSC	ANOVA	$F=360.5$	5.30	<0.001
	HCNSC	ANOVA	$F=127.4$	5.30	<0.001
	HCC	ANOVA	$F=84.1$	5.30	<0.001
	SC	ANOVA	$F=287.9$	5.30	<0.001
	NGI	Kruskal–Wallis	$H=28.6$	5	<0.001

Note. NND — total numerical neuronal density; HCSC — hyperchromatic shriveled cells (neurons); HCNSC — hyperchromatic non-shriveled cells; HCC — hypochromic cells; SC — shadow cells; NGI — neuroglial index; df — degrees of freedom. For the Kruskal–Wallis test, the *H*-statistic is given; for ANOVA, the *F*-statistic is given.

layer V, while a ratio less than 1 indicates greater sensitivity in layer III.

In layer III of the SMC, the Jonkheere-Terpstra test revealed statistically significant monotonic trends for HCSC (Z=–2.98, p=0.001 — decreasing), HCNSC (Z=1.88, p=0.030 — increasing), HCC (Z=2.45, p=0.007 — increasing), and NGI (Z=–4.92, p>0.001 — decreasing). No significant monotonic trends were detected for NND and SC (p>0.05). However, the test for the quadratic component showed high significance for NND (F=16.4, p<0.001), HCNSC (F=8.2, p=0.006), HCC (F=7.4, p=0.009), and SC (F=19.2, p<0.001), confirming the non-monotonic (wave-like) nature of their dynamics. For HCNSC and HCC, a mixed pattern was identified (both components are significant) (Table 4).

In Layer V of the SMC, the Jonkheere-Terpstra test revealed significant monotonic trends for all parameters except NND: HCSC (Z=–2.94, p=0.002 — decreasing), HCNSC (Z=2.30, p=0.011 — increasing), HCC (Z=4.82, p<0.001 — increasing), SC (Z=–3.85, p<0.001 — decreasing), NGI (Z=4.15, p<0.001 — increasing). The quadratic component test was not significant for most parameters (p>0.05), with the exception of HCNSC (p=0.048) and NGI (p=0.028), where a mixed pattern was observed (Table 4).

Strong intralayer correlations were identified in the SMC for layer III: total NND was negatively correlated with all parameters (r ranging from –0.88 to –0.45), SC correlated negatively with NGI (r=–0.70), whereas HCSC, HCNSC, and HCC formed a cluster of positive correlations (r ranging from 0.46 to 0.95) (Table 5.1).

For layers III and V, there was no interlayer correlation for total NND (r=0.08), a moderate positive correlation for HCSC (r=0.52), moderate negative correlations for HCNSC (r=–0.38), HCC (r=–0.39) and SC (r=–0.54), as well as a weak positive correlation with NGI (r=0.35) (Table 5.2).

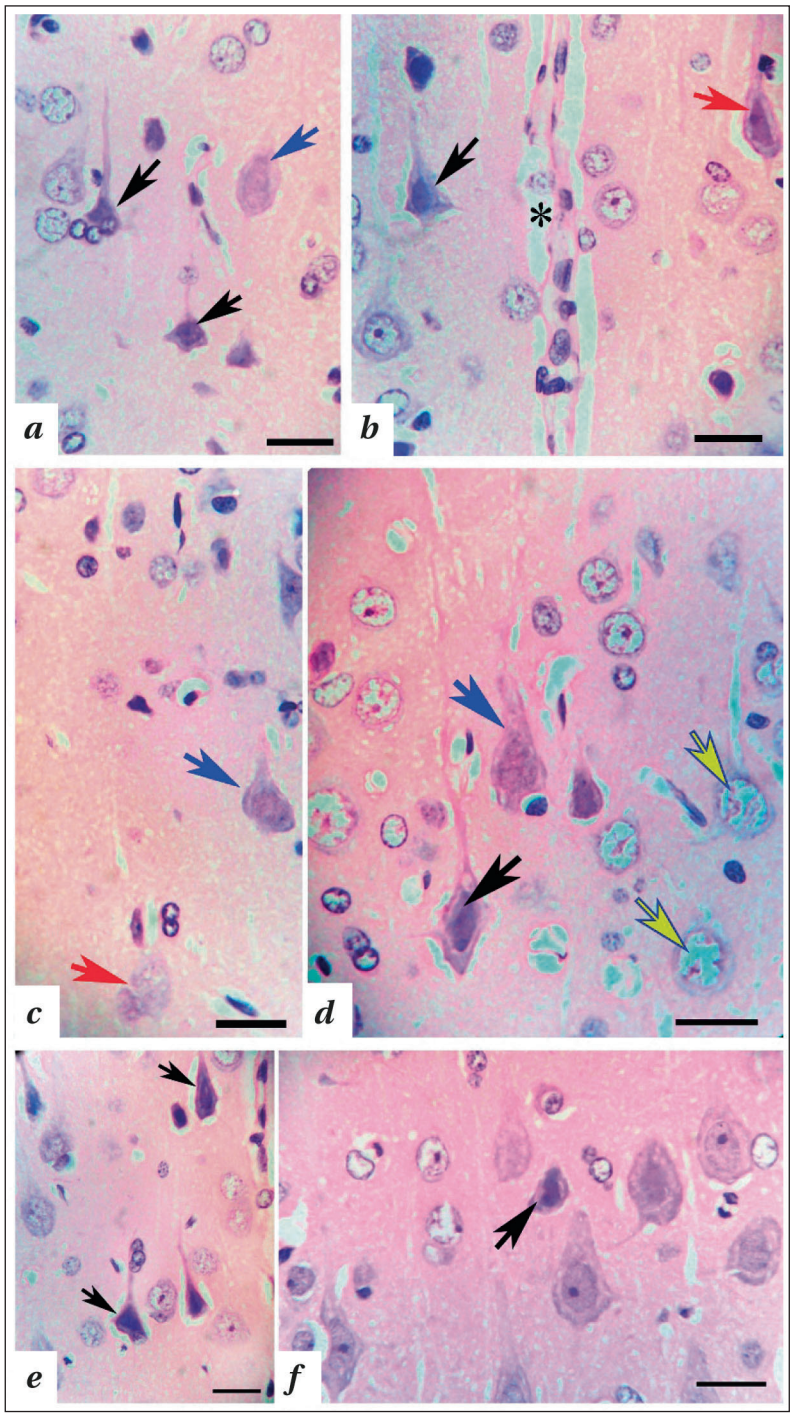

Fig. 2. PReactively altered pyramidal neurons in layer V of the rat sensorimotor cortex following BCCAL.

Note. Hematoxylin-eosin staining. 100× objective, scale bar = 20 µm. *a*, *b* — 30 days after bilateral CCAL. Black arrows — hyperchromatic shreveled neurons. Blue arrow — hypochromatic neurons. Red arrow — vacuolated («red») neurons. * — microvessel with signs of perivascular edema. *c*, *d* — 90 days after bilateral CCAL. Black arrow — hyperchromatic neurons. Blue arrows — hypochromatic neurons. Red arrow — shadow cells. Yellow arrows — signs of edema and swelling of neuropil cell bodies. *e* — 150 days; *f* — 210 days after bilateral CCAL. Black arrows — hyperchromatic neurons.

To assess differences in the dynamics of pathological processes between layers III and V, linear mixed models (LMMs) with a random intercept for the animal were used (Table 6). The «Layer × Time» interaction effect was statistically significant for all six morphometric parameters (p<0.001). The foremost interaction was observed for HCSC (F=71.2), indicating fundamentally different dynamics of irreversible ischemic damage in

Table 2. Reactive neurons at the time points of the study: comparison with controls (2.1) and percentage distribution in layers III and V of the rat sensorimotor cortex (2.2).

2.1. Comparison with control

Layer	Parameter	Time point, day	Difference	95% CI	*p-corr*	η^2_p
III	NND	30	–31.9	[–39.5; –24.3]	< 0.001	0.89
		270	–20.0	[–27.6; –12.4]	< 0.001	
	HCSC	90	+10.4	[8.0; 12.8]	< 0.001	0.91
	HCNSC	30	+8.2	[6.5; 9.9]	< 0.001	0.88
		210	+9.3	[7.6; 11.0]	< 0.001	
	HCC	150	+8.0	[6.6; 9.4]	< 0.001	0.90
	SC	210	+27.0	[24.0; 30.0]	< 0.001	0.94
	NGI	30	+0.84	[0.78; 0.90]	< 0.001	0.95
V	HCSC	30	+10.4	[9.6; 11.2]	< 0.001	0.97
	NGI	270	+0.45	[0.38; 0.52]	< 0.001	0.89

2.2. Interlayer comparison

Time point, day	Parameter	Neurons proportion in layers (% , *Me* [*IQR*])		*p*	*p-corr*
		III	V		
30	HCSC	18.7 [16.5–21.0]	27.4 [25.3–29.6]	0.004	0.016
	HCNSC	23.7 [21.0–25.5]	13.0 [11.5–14.5]	< 0.001	< 0.001
	HCC	4.5 [3.2–5.8]	9.2 [8.0–10.5]	< 0.001	< 0.001
	SC	20.7 [18.0–23.0]	8.8 [7.2–10.9]	< 0.001	< 0.001
90	HCSC	27.2 [24.5–29.0]	19.5 [18.8–20.0]	0.016	0.064
	HCNSC	13.6 [11.5–15.8]	18.7 [16.8–20.0]	0.031	0.124
	HCC	13.2 [11.0–15.0]	13.6 [12.1–14.6]	0.720	> 0.05
	SC	25.9 [20.5–30.0]	15.5 [15.3–15.8]	0.016	0.064
150	HCSC	18.8 [17.0–20.5]	21.9 [20.7–23.1]	0.016	0.064
	HCNSC	13.9 [12.0–15.5]	18.8 [17.8–19.7]	0.004	0.016
	HCC	17.1 [15.0–18.8]	12.8 [10.2–14.6]	0.016	0.064
	SC	26.7 [22.0–31.0]	14.1 [13.1–16.0]	0.004	0.016
210	HCSC	14.9 [13.0–16.5]	21.2 [20.0–21.6]	< 0.001	< 0.001
	HCNSC	18.9 [16.5–21.0]	12.9 [11.1–13.7]	0.004	0.016
	HCC	10.6 [8.5–12.8]	5.9 [5.0–7.2]	0.004	0.016
	SC	30.5 [26.3–32.0]	16.9 [16.0–17.9]	0.004	0.016
270	HCSC	20.6 [18.0–23.0]	22.8 [21.8–23.3]	0.031	0.124
	HCNSC	17.7 [15.5–19.8]	10.4 [9.9–11.5]	< 0.001	< 0.001
	HCC	10.5 [8.8–12.2]	5.7 [5.1–7.1]	0.004	0.016
	SC	37.3 [33.0–41.0]	16.8 [14.0–19.4]	0.004	0.016

Note. NNND — total numerical neuronal density; HCSC— hyperchromatic shriveled cells (neurons); HCNSC — hyperchromatic non-shriveled cells; HCC — hypochromic cells; SC — shadow cells; CI — confidence interval; η^2_p — partial eta-squared (measure of effect size); Me — median; IQR — interquartile range. Percentages were calculated using the formula: (density of a given cell type / NND) × 100%. In Table 2.1, for NND, HCSC (layers III and V), and HCC (layer V), we used Tukey's post-hoc test (ANOVA); for the others, we used Dunn's method with Bonferroni correction (Kruskal–Wallis). In Table 2.2, the Wilcoxon signed-rank test for dependent samples with Bonferroni correction was used for inter-layer comparisons (adjusted significance level $p < 0.005$ for 10 comparisons).

Table 3. Comparative analysis of the vulnerability of layers III and V of the rat sensorimotor cortex at study time points.

Parameters	Layers, % max. changes vs control		Ratio V/III
	III	V	
NND	–44.6 (30 day)	–11.6 (150 day)	0.26
HCSC	+473 (90 day)	+945 (30 day)	2.00
HCNSC	+683 (30 day)	+527 (90 day)	0.77
HCC	+500 (150 day)	+364 (90 day)	0.73
SC	+1800 (210 day)	+455 (90 day)	0.25
NGI	+95.5 (30 day)	+42 (270 day)	0.44

Note. NND — total numerical neuronal density; HCSC — hyperchromatic shriveled cells (neurons); HCNSC — hyperchromatic non-shriveled cells; HCC — hypochromatic cells; SC — shadow cells; NGI — neuroglial index. The maximum percentage change was calculated using the formula: [(maximum parameter value after CCAL — control value) / control value] × 100% (for indicators showing an increase, «+») or [(minimum value after CCAL — control value) / control value] × 100% (for indicators showing a decrease, «–»). A vulnerability ratio > 1 indicates higher sensitivity of layer V, < 1 indicates higher sensitivity of layer III. The time period during which the maximum change was recorded is indicated in parentheses.

the examined layers. △-analysis (consistency of the direction of changes between adjacent time points) showed that for SC, HCSC, and NGI, changes in layers III and V were co-directional significantly more often than by chance (68%, 66%, and 64%, respectively; $p < 0.05$ for all). The highest consistency was observed for SC — a marker of complete neuronal death.

To assess whether one layer might be leading the other, we compared the timing of extreme pa-

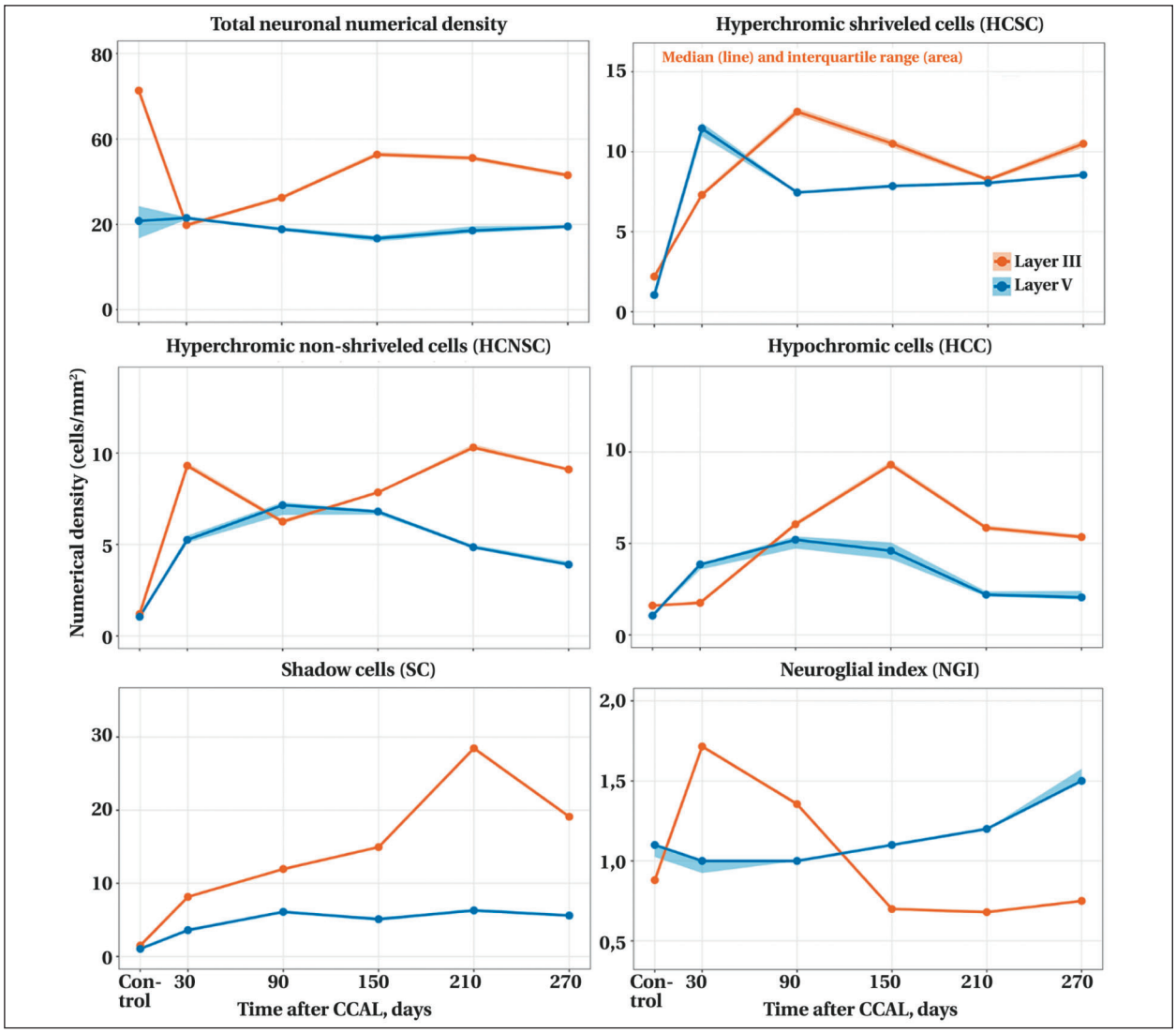

Fig. 3. Comparison of the dynamics of the density of reactive and pathologically altered neurons in layers III and V of the rat sensorimotor cortex at the long-term following ligation of the common carotid arteries.
Note. On the graphs: median — line; interquartile range — box (not shown for minimal values).

rameter values (maxima and minima) in layers III and V of the SMC based on group averages. Synchronization of the extrema — that is, the occurrence of a maximum or minimum at the same time — was observed for the HCSC and for the secondary SC peak. The HCSC peak was recorded in both layers at 30 days; however, in layer V, the damage intensity was +945%, whereas in layer III, the HCSC peak was delayed and less pronounced (90 days, +473%). The secondary SC peak was also synchronous in both layers and recorded at 210 days (layer III: +1800%, layer V: +455%). A temporal priority of layer III, i.e., the onset of the extreme values occurring earlier than in layer V, was identified for total NND, HCNSC and HCC, and NGI. The first minimum of total NND was recorded at 30 days in layer III and at 150 days in layer V. The maximum of HCNSC was reached at 30 days in layer III (+683%) and at 90 days in layer V (+527%). The maximum for HCC was recorded at 150 days in layer III (+500%) and at 90 days in layer V (+364%); meanwhile, in layer III, HCC began to increase as early as 30 days, reaching a plateau by 150 days

The maximum NGI was observed at 30 days in layer III (+95.5%) and at 270 days in layer V (+42%), with the most pronounced lead being 240 days. A temporal priority of layer V was identified only for the first SC peak: 90 days in layer V (+455%) versus 210 days in layer III (+1800%). Analysis of the dynamics of HCNSC and HCC showed that in layer III, HCNSC reaches its maximum early (30 days) followed by a decline, whereas HCC has a delayed peak (150 days). In layer V, both parameters peaked synchronously at 90 days.

Discussion

This study is the first to conduct a comparative analysis of the long-term (up to 270 days) dynamics of reactively altered neurons in layers III and V of the sensorimotor cortex in a model of chronic cere-

Table 4. Results of the Jonckheere-Terpstra test and the quadratic trend test.

Layer	Parameter	*Z*	*p* (Jonckheere)	Trend	*F* (quad.)	*p* (quad.)	pattern
III	NND	3.12	0.999	нет	16.4	< 0.001	non-monotonic
	HCSC	–2.98	0.001	МУ	1.8	0.185	linear
	HCNSC	1.88	0.030	МВ	8.2	0.006	mixed
	HCC	2.45	0.007	МВ	7.4	0.009	mixed
	SC	–1.35	0.088	нет	19.2	< 0.001	non-monotonic
	NGI	–4.92	< 0.001	МУ	2.1	0.152	linear
V	NND	–1.02	0.154	нет	0.8	0.382	no trend
	HCSC	–2.94	0.002	МУ	3.2	0.079	linear
	HCNSC	2.30	0.011	МВ	4.1	0.048	mixed
	HCC	4.82	< 0.001	МВ	0.9	0.347	linear
	SC	–3.85	< 0.001	МУ	2.9	0.094	linear
	NGI	4.15	< 0.001	МВ	5.1	0.028	mixed

Note. NND — total numerical neuronal density; HCSC — hyperchromatic shriveled cells (neurons); HCNSC — hyperchromatic non-shriveled cells; HCC — hypochromatic cells; SC — shadow cells; NGI — neuroglial index. The Jonkheere–Terpstra test checks for the presence of a monotonic (constantly increasing or constantly decreasing) trend. A positive *Z*-value indicates an increasing trend, while a negative value indicates a decreasing trend. The quadratic trend test was performed using Kruskal–Wallis rank-sum analysis with orthogonal polynomials. MD — monotonically decreasing; MI — monotonically increasing.

Table 5. Pearson correlation matrices (r) between the intra- (5.1) and inter-layer (5.2) parameters of the rat sensorimotor cortex following ligation of the common carotid arteries.

5.1. Correlations between parameters in layer III ($p < 0.05$)

Parameters	*R* values for the compared parameters				
	HCSC	**HCNSC**	**HCC**	**SC**	**NGI**
NND	**–0.84**	**–0.82**	**–0.85**	**–0.45**	**–0.88**
HCSC		**0.78**	**0.76**	**0.52**	**0.68**
HCNSC			**0.95**	**0.48**	**0.75**
HCC				**0.46**	**0.74**
SC					**–0.70**

5.2. Correlations between the same parameters in layers III and V

Parameters	*r* (III and V)	*p*
NND	0.08	0.64
HCSC	**0.52**	**0.001**
HCNSC	**–0.38**	**0.02**
HCC	**–0.39**	**0.02**
SC	**–0.54**	**< 0.001**
NGI	**0.35**	**0.04**

Note. Statistically significant correlations ($p < 0.05$) are shown in bold, ($n = 36$ paired observations).

Table 6. Analysis of the connections between layers III and V of the rat sensorimotor cortex.

6.1. Two-factor LMM with a random intercept for the Animal (the «Layer × Time» interaction effect)

Parameters	*F*	df1	df2	*p*
NND	38.4	5	29.1	< 0.001
HCSC	71.2	5	28.9	< 0.001
HCNSC	36.8	5	29.0	< 0.001
HCC	30.5	5	29.2	< 0.001
SC	24.1	5	28.8	< 0.001
NGI	28.6	5	29.0	< 0.001

6.2. Correlation and △-analysis

Parameters	Correlation *r* (95% CI)	Partial *r*	Consistency, %	*p*
SC	0.58 [0.31; 0.76]	0.52	68	0.004
HCSC	0.52 [0.23; 0.73]	0.48	66	0.008
NGI	0.44 [0.14; 0.67]	0.37	64	0.016

Note. NND — total numerical neuronal density; HCSC — hyperchromatic shriveled cells (neurons); HCNSC — hyperchromatic non-shriveled cells; HCC — hypochromatic cells; SC — shadow cells; NGI — neuroglial index; LMM (Linear Mixed Model) — a linear mixed model with a random intercept for the «Animal» factor: Parameter ~ Layer × Time + (1 | Animal); df — degrees of freedom (according to Satterwhite); partial correlation — controlling for the «Time» factor; △-analysis was performed on 80 pairs of changes (4 time points × 20 animals); binomial test vs. null hypothesis of 50% agreement.

bral ischemia (bilateral CCAL) using appropriate statistical methods that account for pairwise dependence (linear mixed models with random intercepts for the animal) and the limitations of a small number of time points—in favor of △-analysis and analysis of extrema. Chronic ischemia, unlike acute infarction, more often causes progressive dysfunction and dystrophy rather than massive coagulative necrosis [1, 3, 11]. Therefore, the prioritized classification and grading of altered neurons, taking into account the specifics of the bilateral CCAL model, had their own distinctive features.

The morphological picture following bilateral CCAL revealed a spectrum of changes — ranging

from potentially reversible dystrophic changes (atrophy, vacuolization) to irreversible necrobiotic changes (coagulative necrosis, lysis) — which supported the model of progressive neurodegeneration under conditions of chronic cerebral hypoperfusion. The detection of «red neurons» in the long-term indicated a dynamic, progressive nature of the damage, in which acute ischemic episodes superimposed on the chronic process. Meanwhile detection of hypertrophied neurons indicated concomitant compensatory-plastic processes. This morphological mosaic reflected the competition between two pathogenetic trends: destructive (neurodegeneration) and adaptive (neuroplasticity). Preservation of the pool of hypertrophied neurons may have represented a structural reserve of the cortex and a morphological substrate for partial functional recovery, which explained the clinical variability of neurological deficits in chronic cerebral ischemia.

According to our data, layer III proved to be more sensitive to neuronal loss, the accumulation of reversible dystrophic forms (HCNSC, HCC), and delayed death (SC), whereas layer V was characterized by a selectively high vulnerability to irreversible ischemic damage leading to emergence of the hyperchromatic shriveled (HCSC) neuron type. A biphasic decrease in NND in layer III with wave-like dynamics (quadratic trend, $F=16.4$, $p<0.001$) indicated damage with partial recovery and delayed secondary degeneration, which is consistent with the concept of dissociative neurodegeneration in chronic ischemia [8]. The first phase of the decrease (by 44.6% at 30 days, $p<0.001$) reflected the direct consequences of acute hypoperfusion and an energy crisis.

The subsequent partial recovery (150–210 days, NND 55.6–56.3 cells/ mm²) may have been associated with adaptation and compensatory mechanisms, including the plasticity of surviving neurons and temporary functional-spatial reorganization of neural networks. The final decrease in NND by 270 days (to 51.5 cells/ mm², –28.0% of control) indicated the exhaustion of compensatory potential and development of delayed secondary degeneration. NND decrease was less evident in layer V (maximum –11.6% at 150 days, $p=0.048$) and did not show a statistically significant trend (Jonkheere–Terpstra test, $p=0.154$; quadratic component, $p=0.382$). This corresponds to a model of slowly progressive atrophy without pronounced recovery waves.

Thus, layer III was characterized by non-monotonic (wave-like) dynamics of NND, HCNSC, HCC, and SC, reflecting processes of partial recovery and delayed degeneration. In contrast, layer V was characterized by linear (monotonic) dynamics of most parameters, which corresponded to a model of slowly progressive atrophy without marked compensation waves. The most obvious difference between the layers was observed for SC: in layer III — a non-monotonic pattern with a delayed peak (210 days); in layer V — a monotonic decline following an early peak (90 days).

The extreme increase in HCSC in layer V at 30 days (945% higher than the control) confirmed high metabolic vulnerability of the large pyramidal neurons of the corticospinal tract [7]. The V/III layers vulnerability ratio based on HCSC was 2.00, indicating a significantly higher sensitivity of layer V to irreversible ischemic damage. The «dark neuron» phenomenon is traditionally regarded as a marker of severe, often irreversible ischemic damage [11, 13]. A monotonically HCSC decreasing trend in layer V ($Z=-2.94$, $p=0.002$) indicated gradual elimination of these cells following acute injury. In layer III, by contrast, the peak of HCSC was delayed until 90 days and was less pronounced (+473%), which may indicate a slower development of coagulative necrosis in the superficial layers.

HCNSC and HCC dominated in layer III, but their dynamics differed fundamentally. HCNSC peaked at 30 days (+683%), reflecting an acute response to ischemic stress characterized by protein overexpression and preservation of cellular architecture [14–16]. HCC, in contrast, had a delayed peak at 150 days (+500%), indicating increasing suppression of protein synthesis and chromatolysis as compensatory mechanisms were exhausted. The temporal disparity between HCNSC and HCC peaks is a novel, not described previously phenomenon, indicating that hyperchromic and hypochromic responses represent not merely different stages of a single process, but qualitatively distinct mechanisms of response to chronic ischemia. The wave-like dynamics of HCNSC (quadratic trend, $F=8.2$, $p=0.006$) and HCC mixed pattern (monotonically increasing trend, $Z=2.45$, $p=0.007$; quadratic component, $F=7.4$, $p=0.009$) indicated a recurrent nature of functional disruptions with periods of compensation and decompensation. In layer V, both parameters peaked synchronously at 90 days (HCNSC: +527%, HCC: +364%), which may indicate a more rapid depletion of metabolic reserves in the deep layers.

The dynamics of shadow cells — a marker of complete neuronal death — deserve special attention. In layer III, SC exhibited a non-monotonic pattern with a delayed peak at 210 days (quadratic trend, $F=19.2$, $p<0.001$; maximum increase of +1800% compared to control). In layer V, the SC peak was recorded earlier (90 days, +455% compared to control), followed by a monotonically decreasing trend ($Z=-3.85$, $p<0.001$). This difference may indicate different mechanisms of neuronal death: in layer III — delayed secondary degeneration occurring after the exhaustion of compensatory mechanisms; in layer V — earlier elimination of dead cells, directly associated with the extreme accumulation of HCNSC at 30 days.

The results indicate that neuronal loss in different layers occurred independently, whereas the accumulation of HCNSC was moderately synchronous. Negative interlayer correlations for HCNSC (r=–0.38), HCC (r=–0.39), and SC (r=–0.54) may indicate a redistribution of functional load between layers or an alternative pattern of complete degeneration (predominant damage to either layer III or layer V in different animals). Neuronal death in layer V occurred earlier, which may be a direct consequence of the extreme accumulation of HCNSC at 30 days. In layer III, neuronal death (SC) was delayed until day 210, which corresponds to the model of secondary degeneration following the exhaustion of compensatory mechanisms [8, 17, 18].

The diverse nature of the injury was confirmed by the dynamics of NGIs. Early transient gliosis in layer III (peaking at 30 days, +95.5% compared to control, followed by a steady decline, Z=–4.92, $p<0.001$) corresponded to the classical model of an acute astroglial reaction with possible involvement of astrocytes in neuroprotection and recovery of homeostasis [19, 20]. In contrast, a sustained increase in NGI in layer V over 270 days (maximum +42% by day 270, mixed pattern: monotonically increasing trend Z=4.15, $p<0.001$; quadratic component F=5.1, p=0.028) indicated a chronic neuroinflammatory process and prolonged glial activation, which over time may contribute to the progression of degeneration [19–21]. A statistically significant «Layer × Time» interaction for NGI (F=28.6, $p<0.001$) confirmed fundamentally different temporal dynamics of gliosis in analyzed layers.

Contrary to the initial hypothesis of a cascade-like spread of degeneration from superficial layers to deeper ones, the data from the analysis of reactively altered neurons did not confirm a directional (lag-like) influence between the layers of the SMC. Correlation analysis at the individual animal level (n=36) revealed statistically significant positive correlations between layers for the SC (r=0.58; 95% CI [0.31; 0.76]; $r\_partial$=0.52; p=0.004), HCSC (r=0.52; [0.23; 0.73]; $r\_partial$=0.48; p=0.008), and NGI (r=0.44; [0.14; 0.67]; $r\_partial$=0.37; p=0.016). High values of partial correlations (with the control of «Time» factor) indicated intragroup consistency — in the same animals, degenerative processes in different layers proceed synchronously.

△-analysis (consistency of the direction of changes between adjacent time points) showed that for SC, HCSC, and NGI, changes in layers III and V were in the same direction significantly more often than would be expected by chance: for SC — 68% (55 out of 80, p=0.004), for HCSC — 66% (53 out of 80, p=0.008), for NGI — 64% (51 out of 80, p=0.016). The highest consistency was observed for SC — a marker of complete neuronal death. Thus, according to the analysis of the numerical density of reactively altered neurons, pathological processes in layers III and V developed in parallel and moderately synchronously, rather than sequentially. This did not rule out the presence of complex network interactions between layers, but did not confirm the simple cascade model of «first layer III, then layer V».

A comparison of the times of the extrema revealed different patterns of temporal dynamics in layers III and V. Synchrony was observed for the HCSC (peak at 30 days in both layers) and for the secondary SC peak (210 days in both layers). For HCSC, this confirmed the simultaneous development of acute ischemic injury; however, the intensity of this damage was significantly higher in layer V (+945% versus +473% in layer III, where the peak occurred at 90 days), which is consistent with the high metabolic vulnerability of large pyramidal neurons of the corticospinal tract [7].

A temporal priority of layer III was identified for most parameters reflecting neuronal functional state (NND, HCNSC) and glial response (NGI). The first minimum of NND was recorded at 30 days in layer III and at 150 days in layer V. The maximum of HCNSC was reached at 30 days in layer III and at 90 days in layer V. The most pronounced advance (at 240 days) was observed for NGI: an early transient peak in layer III (30 days, +95.5%) and a late prolonged peak in layer V (270 days, +42%). According to the literature, this likely indicates different mechanisms of the glial response: neuroprotective astroglial activation in the superficial layers and chronic neuroinflammation in the deep layers [22–24]. For HCC, a predominance of layer V was identified (peak at 90 days versus 150 days in layer III), which may reflect a more rapid depletion of metabolic reserves in the deep layers.

A temporal priority of layer V was also observed for the first SC peak (90 days vs. 210 days). This implies that complete neuronal death in the deep layers occurred earlier, which may be a direct consequence of the extreme accumulation of HCSC in layer V at 30 days. In layer III, neuronal death was delayed until 210 days, which is consistent with a model of secondary degeneration following the exhaustion of compensatory mechanisms [8, 17, 18].

Thus, the analysis of extrema confirmed that pathological processes in layers III and V did not develop completely synchronously: functional disruptions (HCNSC) and the glial response occurred earlier in layer III, whereas complete neuronal death (SC) and the depletion of metabolic reserves (HCC) occurred earlier in layer V. However, for the key marker of irreversible damage (HCSC), synchrony was observed in terms of timing, but with varying intensity and a delayed peak in layer III.

The results obtained are consistent with studies demonstrating the heterogeneity of damage to cor-

tical layers during ischemia [10, 22–26], but for the first time they demonstrate long-term dynamics (up to 270 days) in a model of chronic hypoperfusion using appropriate statistical methods that account for individual variability. In contrast to data obtained in the acute ischemia model [11, 18, 27–29], massive coagulative necrosis was not observed; instead, progressive dystrophy with polymorphism of reactive changes dominated, which corresponded to the chronic nature of the injury and the model's characteristics — the presence of a well-developed collateral network in rodents. In addition, the small number of time points (6) limited the ability to identify complex nonlinear relationships, although the use of quadratic trends partially compensated for this limitation.

Conclusion

Chronic cerebral ischemia induced by bilateral ligation of the common carotid arteries led to statistically significant and qualitatively distinct changes in neuronal populations in layers III and V of the rat cerebral cortex during the long-term follow-up period (up to 270 days).

Layer III of the SMC was characterized by a biphasic decrease in total neuronal density (peaking at 30 days), asynchronous dynamics of hyperchromatic non-shriveled (peaking at 30 days) and hypochromatic neurons (peaking at 150 days) (quadratic trends), a delayed peak in shadow cells (210 days), and transient gliosis (peaking at 30 days, followed by a decline). This reflected a damage model featuring components of partial recovery and delayed secondary degeneration.

Layer V of the SMC was characterized by a less pronounced but sustained decrease in the overall neuronal density (peaking at 150 days, with no significant trend), an extreme early increase in hyperchromic shrunken neurons (day 30, which was twice the increase in layer III), a synchronous peak of hyperchromatic non-shriveled and hypochromatic neurons (day 90), monotonous depletion of hypochromatic neurons (linear increasing trend), an early peak of shadow cells (90 days), and prolonged progressive gliosis (by 270 days). This corresponded to a model of progressive degeneration with primary metabolic damage to large pyramidal neurons.

Linear mixed models with random intercepts for each animal confirmed the presence of a statistically significant interaction between the «Layer» and «Time» factors for all key morphometric parameters, demonstrating different temporal dynamics of pathological processes in the layers under study.

Correlation analysis at the individual animal level revealed moderate positive correlations between layers. △-analysis showed consistency in changes for shadow cells, hyperchromatic shriveled neurons, and the neuroglial index. The time points of the peaks for hyperchromatic shriveled neurons (30 days) and the secondary peak of shadow cells (210 days) were synchronous in both layers. A temporal priority of layer III of the SMC was detected for the total neuronal density, hyperchromatic non-shriveled neurons, and the neuroglial index (early time points). A temporal priority of layer V was identified for the first peak of shadow cells and hypochromatic neurons. No conclusive evidence of a cascade-like spread of damage from superficial to deep layers was obtained, with the exception of a possible lead in the glial reaction in layer III of the SMC.

The data obtained support the need for further comparative studies of layers III and V of the SMC in a larger sample of animals and for the development of therapeutic strategies aimed at both protecting metabolically vulnerable pyramidal neurons and modulating the glial response during chronic hypoperfusion.

References

1. *Iadecola C.* The pathobiology of vascular dementia. *Neuron.* 2013; 80 (4): 844–866. DOI: 10.1016/j.neuron.2013.10.008. PMID: 24267647.
2. *Morgan A. E., Mc Auley M. T.* Vascular dementia: from pathobiology to emerging perspectives. *Ageing Res Rev.* 2024; 96: 102278. DOI: 10.1016/j.arr.2024.102278. PMID: 38513772.
3. *Kalaria R.N.* The pathology and pathophysiology of vascular dementia. *Neuropharmacol.* 2018; 134 (Pt B): 226–239. DOI: 10.1016/j.neuropharm.2017.12.030. PMID: 29273521.
4. *Zhang X., Chang S., Liu J., Wang D.* Combined metabolomics and proteomics analysis of vascular cognitive impairment in hypertensive rats induced by endothelial injury. *PLoS One.* 2025; 20 (10): e0332827. DOI: 10.1371/journal.pone.0332827. PMID: 41066429.
5. *Schaechter J.D., Perdue K.L.* Enhanced corticospinal tract fiber integrity and motor recovery following stroke evidenced by diffusion tensor imaging. *Neurorehabil Neural Repair.* 2008; 22 (6): 758–772. DOI: 10.1177/1545968308317530.
6. *DeFelipe J.* The anatomical problem posed by brain complexity and size: a potential solution. *Front Neuroanat.* 2015; 9: 104. DOI: 10.3389/fnana.2015.00104. PMID: 26347617.
7. *Zhang S., Murphy T.H.* Imaging the impact of cortical microcirculation on synaptic structure and sensory-evoked hemodynamic responses *in vivo. PLoS Biol.* 2007; 5 (5): e119. DOI: 10.1371/journal.pbio.0050119. PMID: 17456007.
8. *Carmichael S.T.* Brain excitability in stroke: the yin and yang of stroke progression. *Arch Neurol.* 2012; 69 (2): 161–167. DOI: 10.1001/archneurol.2011.1175. PMID: 21987395.
9. *Kalinichenko S.G., Korobtsov A.V., Matveeva N.Yu., Pushchin I.I.* Structural and chemical changes in glial cells in the rat neocortex induced by constant occlusion of the middle cerebral artery. *Acta Histochem.* 2020; 122 (5): 151573. DOI: 10.1016/j.acthis.2020.151573. PMID: 32622419.
10. *Zhang X., Wei M., Fan J., Yan W., Zha X., Song H., Wan R., Yin Y., Wang W.* Ischemia-induced upregulation of autophagy preludes dysfunctional lysosomal storage and associated synaptic impairments in neurons. *Autophagy.* 2021; 17 (6): 1519–1542. DOI: 10.1080/15548627.2020.1840796. PMID: 33111641.
11. *Авдеев Д.Б., Степанов С.С., Горбунова А.В., Шоронова А.Ю., Макарьева Л.М., Акулинин В.А., Коржук М.С. с соавт.* Темные нейроны сенсомоторной коры белых крыс после острой неполной ишемии в аспекте артефактов фиксации и нейроглиальных взаимоотношений. *Журнал анатомии и гистопатологии.* 2021; 10 (2): 9–22. *Avdeev D.B., Stepanov S.S., Gorbunova A.V., Shoronova A.Yu., Makaryeva L.M., Akulinin V.A., Korzhuk M.S., et al.* Dark neurons of the sensorimotor cortex of white rats after acute incomplete ischemia in terms of fixation artifacts and neuroglial relationships. *Journal of Anatomy and Histopathology = Zhurnal Anatomiya i Gistopatologiya.* 2021; 10 (2): 9–22. (in Russ.). DOI: 10.18499/2225-7357-2021-10-2-9-22.
12. *Pekny M., Pekna M.* Astrocyte reactivity and reactive astrogliosis: costs and benefits. *Physiol Rev.* 2014; 94 (4): 1077–1098. DOI: 10.1152/physrev.00041.2013. PMID: 25287860.
13. *Зиматкин С.М., Бонь Е.И.* Темные нейроны мозга. *Морфология.* 2017; 152 (6): 81–86. *Zimatkin S. M., Bon E. I.* Dark neurons of the brain. *Morphollogy = Morfologiya.* 2017; 152 (6): 81–86. (in Russ.). DOI: 10.17816/morph.398200.
14. *Brown G.C.* Neuronal loss after stroke due to microglial phagocytosis of stressed neurons. *Int J Mol Sci.* 2021; 22 (24): 13442. DOI: 10.3390/ijms222413442. PMID: 34948237.
15. *Chen S., Shao L., Ma L.* Cerebral edema formation after stroke: emphasis on blood–brain barrier and the lymphatic drainage system of the brain. *Front Cell Neurosci.* 2021; 15: 716825. DOI: 10.3389/fncel.2021.716825. PMID: 34483842.
16. *Kalinichenko S.G., Pushchin I.I., Matveeva N.Yu.* Neurotoxic and cytoprotective mechanisms in the ischemic neocortex. *J Chem Neuroanat.* 2023; 128: 102230. DOI: 10.1016/j.jchemneu.2022.102230. PMID: 36603664.
17. *Hu C., Chen X., Wang M., Zhang L., Gao D., Zang L.* Analgecine protects against cerebral ischemia-reperfusion through apoptosis inhibition and anti-neuroinflammation in rats. *Neuropeptides.* 2022; 93: 102230. DOI: 10.1016/j.npep.2022.102230. PMID: 35378359.
18. *Behrouzifar S., Esmaily H.* The biological efficacy of Apelin against focal transient cerebral ischemia-reperfusion injury. A systematic review and meta-analysis of animal studies. *Brain Res.* 2024; 15: 1833: 148887. DOI: 10.1016/j.brainres.2024.148887. PMID: 38552935.

19. *Sofroniew M.V.* Astrocyte barriers to neurotoxic inflammation. *Nat Rev Neurosci*. 2015; 16 (5): 249–263.
DOI: 10.1038/nrn3898. PMID: 25891508.
20. *Wilson D.M., Cookson M.R., Van Den Bosch L., Zetterberg H., Holtzman D.M., Dewachter I.* Hallmarks of neurodegenerative diseases. *Cell*. 2023; 186: 693–714.
DOI: 10.1016/j.cell.2022.12.032. PMID: 36803602.
21. *Delgado-Martín S., Martínez-Ruiz A.* The role of ferroptosis as a regulator of oxidative stress in the pathogenesis of ischemic stroke. *FEBS Lett*. 2024; 598 (17): 2160–2173.
DOI: 10.1002/18733468.14894. PMID: 38676284.
22. *Wang X., Zhang X.Y., Liao N. Q., He Z.H., Chen Q.F.* Identification of ribosome biogenesis genes and subgroups in ischaemic stroke. *Front Immunol*. 2024; 15: 1449158.
DOI: 10.3389/fimmu.2024.1449158.
PMID: 39290696.
23. *Голубев А. М.* Морфологическая классификация повреждений нейронов. *Общая реаниматология*. 2025; 21 (5): 4–14. *Golubev A.M.* Morphological classification of neuronal damage. *General Reanimatology = Obshchaya Reanimatologiya*. 2025; 21 (5): 4–14. (in Russ. & Eng.). DOI: 10.15360/1813-9779-2025-5-2580.
24. *Sheikh A., Meng X., Kao J.P.Y, Kanold P.O.* Neonatal hypoxia-ischemia causes persistent intracortical circuit changes in layer 4 of rat auditory cortex. *Cereb Cortex*. 2022; 32 (12): 2575–2589.
DOI: 10.1093/cercor/bhab365.
PMID: 34729599.
25. *Chen J.-M., Shi G., Yu Lu-Lu., Shan W., Sun J.-Yu, Guo A.-C., Wu J.-P., Tang T.-S., Zhang X.-J., Wang Q.* 3-HKA promotes vascular remodeling after stroke by modulating the activation of A1/A2 reactive astrocytes. *Adv Sci (Weinh)*. 2025; 12 (11): e2412667.
DOI: 10.1002/advs.202412667.
PMID: 39854137.
26. *Yanumula A., Cusick J. K.* Biochemistry, extrinsic pathway of apoptosis. In: StatPearls [Internet]. Treasure Island (FL): StatPearls Publishing; 2025. PMID: 32809646 Free Books & Documents.
27. *Бонь Е.И., Максимович Н.Е., Карнюшко О.А., Зиматкин С.М., Новак А.А.* Изменения содержания bcl-2 в теменной коре и гиппокампе крыс при ишемии головного мозга различной степени тяжести. *Новости медико-биологических наук*. 2025; 25 (2): 42–47. *Bon E.I., Maksimovich N.E., Karnyushko O.A., Zimatkin S.M., Novak A.A.* Changes in content of bcl-2 in the parietal cortex and hippocampus of rats with cerebral ischemia of varying severity *News of Biomedical Sciences=Novosti Mediko-biologicheskih Nauk*. 2025; 25 (2): 42–47. (in Russ.).
28. *Боева Е.А., Калабушев С.Н., Варнакова Л.А., Любомудров М.А., Цоколаева З.И., Кузовлев А.Н., Мороз В.В. с соавт.* Аргон-кислородная смесь как мультисистемная терапия после остановки кровообращения: экспериментальное исследование. *Общая реаниматология*. 2026; 22 (1): 26–40. *Boeva E.A., Kalabushev S.N., Varnakova L.A., Lyubomudrov M.A., Tsokolayeva Z.I., Kuzovlev A.N., Moroz V.V., et al.* Argon-oxygen mixture as a multisystem therapy after circulatory arrest: an experimental study. *General Reanimatology = Obshchaya reanimatologiya*. 2026; 22 (1): 26–40. (in Russ. & Eng.). DOI: 10.15360/1813-9779-2026-1-2618.
29. *Song W., Teng L., Wang H., Pang R., Liang R., Zhu Z.* Exercise preconditioning increases circulating exosome miR-124 expression and alleviates apoptosis in rats with cerebral ischemia-reperfusion injury. *Brain Res*. 2025; 15: 1851: 149457.
DOI: 10.1016/j.brainres.2025.149457.
PMID: 39824375.

Received 18.02.2026
Accepted 13.05.2026
Online First 04.06.2026